Catalytic Mechanism of the Cyclohydrolase Activity of Human Aminoimidazole Carboxamide Ribonucleotide Formyltransferase/Inosine Monophosphate Cyclohydrolase†

James M. Vergis‡,§ and G. Peter Beardsley*,‖

Department of Molecular Biophysics and Biochemistry, Yale University, New Haven, Connecticut 06520, and Departments of Pharmacology and Pediatrics, Yale University School of Medicine, New Haven, Connecticut 06520

Received July 2, 2003; Revised Manuscript Received November 24, 2003

ABSTRACT: The bifunctional enzyme aminoimidazole carboxamide ribonucleotide transformylase/inosine monophosphate cyclohydrolase (ATIC) is responsible for catalysis of the last two steps in the *de novo* purine pathway. Using recently determined crystal structures of ATIC as a guide, four candidate residues, Lys66, Tyr104, Asp125, and Lys137, were identified for site-directed mutagenesis to study the cyclohydrolase activity of this bifunctional enzyme. Steady-state kinetic experiments on these mutants have shown that none of these residues are absolutely required for catalytic activity; however, they strongly influence the efficiency of the reaction. Since the FAICAR binding site is made up mostly of backbone interactions with highly conserved residues, we postulate that these conserved interactions orient FAICAR in the active site to favor the intramolecular ring closure reaction and that this reaction may be catalyzed by an orbital steering mechanism. Furthermore, it was shown that Lys137 is responsible for the increase in cyclohydrolase activity for dimeric ATIC, which was reported previously by our laboratory. From the experiments presented here, a catalytic mechanism for the cyclohydrolase activity is postulated.

The 10 steps of the *de novo* purine biosynthetic pathway are the primary means for providing a supply of purine nucleotides during cell growth and replication in all nonparasitic organisms (*2*, *3*). The dependence of actively dividing cells on purines has made this pathway an appealing target for the development of cancer chemotherapeutics. In all organisms studied to date, except for one known example in *Methanococcus jannaschii* (*4*), the last two steps of this pathway are catalyzed by a single bifunctional protein known as aminoimidazole carboxamide ribonucleotide transformylase/inosine monophosphate cyclohydrolase (ATIC)[1] (Figure 1). The penultimate step, catalyzed by the 5-aminoimidazole-4-carboxamide ribonucleotide transformylase (AICAR TFase) activity, involves a one-carbon transfer from the reduced folate substrate (6*R*)-N^{10}-formyltetrahydrofolate (10-f-FH_4) to the exocyclic amino group of 5-aminoimidazole-4-carboxamide ribonucleotide (AICAR) to form 5-formylaminoimidazole-4-carboxamide ribonucleotide (FAICAR). The final step of the pathway, catalyzed by the inosine monophosphate cyclohydrolase (IMPCHase) activity, involves the formation of inosine 5′-monophosphate (IMP) via the ring closure reaction of FAICAR and the loss of a water molecule. This ring closure reaction completes the formation of the purine ring system.

Prior to the availability of any structural information about ATIC, an IMPCHase catalytic mechanism was proposed by Szabados *et al*. (*5*) which involved catalysis by cysteine, histidine, and an unknown basic residue. Recently, two crystal structures of avian ATIC have been reported (*6*, *7*) in addition to a structure of human ATIC (*1*). The apo structure of avian ATIC was determined to 1.75 Å resolution (*7*); the avian ATIC structure complexed with AICAR and XMP was determined to 1.93 Å resolution (*6*), and the native structure of human ATIC was determined to 1.9 Å resolution (*1*). Both native structures had a purine nucleotide bound in the presumptive IMPCHase active site which was carried along through the purification (*1*, *7*). This purine found in the apo avian structure was identified as xanthosine 5′-monophosphate (XMP) by our laboratory (described below). All of these structures are dimers formed from two identical monomer subunits of ATIC. Our previous studies of the oligomeric state of human ATIC have demonstrated that ATIC exists in a monomer−dimer equilibrium in solution. These studies have also shown that the dimeric form is required for AICAR TFase activity, while both the monomeric and dimeric forms possess IMPCHase activity, with the dimeric form being more active than the monomeric form (*8*). Figure 2 shows the putative IMPCHase active site and

† This work was supported by National Institutes of Health Grant P01 CA 63536.

* To whom correspondence should be addressed: LMP 3096A, P.O. Box 208064, 333 Cedar St., New Haven, CT 06520-8064. Telephone: (203) 785-7305. Fax: (203) 737-2228. E-mail: g.beardsley@yale.edu.

‡ Yale University.

§ Current address: Department of Molecular Physiology and Biological Physics, University of Virginia, Charlottesville, VA 22908-0736.

‖ Yale University School of Medicine.

[1] Abbreviations: 10-f-FH_4, (6*R*)-N^{10}-formyltetrahydrofolate; AICAR, 5-aminoimidazole-4-carboxamide ribonucleotide; AICAR TFase, 5-aminoimidazole-4-carboxamide ribonucleotide transformylase; ATIC, aminoimidazole carboxamide ribonucleotide transformylase/inosine monophosphate cyclohydrolase; FAICAR, 5-formylaminoimidazole-4-carboxamide ribonucleotide; GMP, guanosine 5′-monophosphate; IMP, inosine 5′-monophosphate; IMPCHase, inosine monophosphate cyclohydrolase; XMP, xanthosine 5′-monophosphate.

10.1021/bi035139b CCC: $27.50
Published on Web 01/14/2004

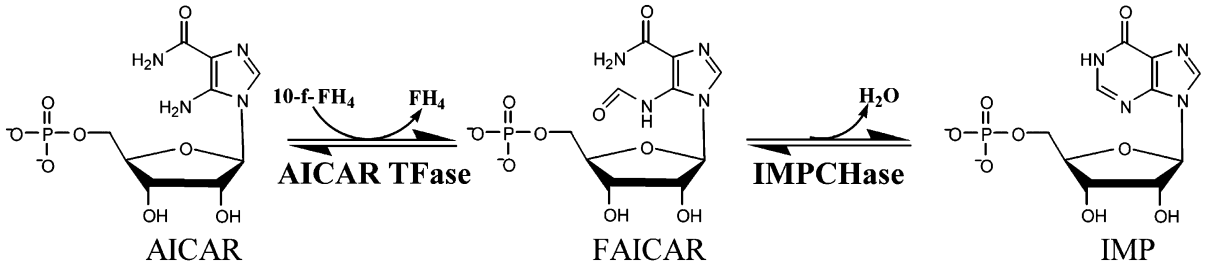

FIGURE 1: Two reactions catalyzed by ATIC.

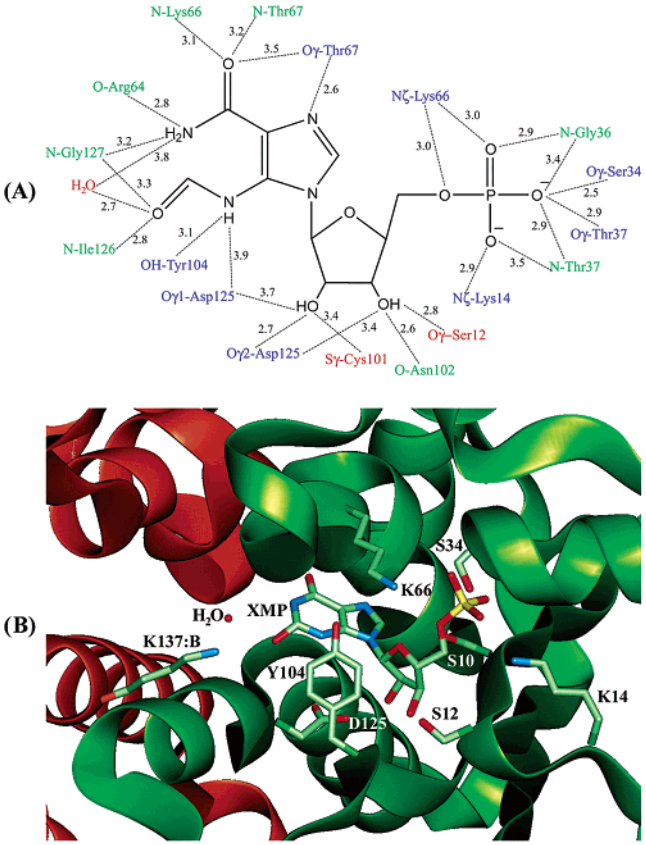

FIGURE 2: (A) Interactions of FAICAR within the IMPCHase active site. The distances are given in angstroms. Conserved backbone interactions are labeled in green; conserved side chain interactions are labeled in blue, and semiconserved interactions are labeled in red. (B) Ribbon diagram showing the IMPCHase active site constructed from the published avian crystal structure. Residues are numbered on the basis of the human sequence. The monomers are colored green and orange.

predicted interactions with its natural substrate, FAICAR, based upon the 1.75 Å resolution structure. On the basis of this structural information, the previously proposed mechanism (*5*) must now be regarded as untenable since the amino acid residues that are implicated are not present near the IMPCHase active site. In the active site region, there are numerous potential interactions between FAICAR and the peptide backbone and two potentially important side chain interactions, involving Tyr104 and Asp125. It is also hypothesized that Lys66 may be an important residue for catalysis despite the fact it is predicted to be located more than 5.5 Å from the amide and formyl groups on FAICAR, where the cyclization reaction occurs. However, Lys66 is within 3.5 Å of the hydroxyl group on Tyr104. Lastly, an additional interaction arises from Lys137, located on the other monomer of ATIC, by way of a water molecule conduit. Since the monomeric form of ATIC suffices for IMPCHase activity, Lys137 is not essential for catalysis. However, this interaction may explain the marked increase in IMPCHase activity observed in dimeric ATIC.

In this study, we have utilized site-directed mutagenesis and steady-state kinetics to probe the residues involved in catalyzing the IMPCHase reaction and used these results to postulate a catalytic mechanism for this activity. The conclusions and mechanism presented in this paper agree with those derived from an independent, detailed structure analysis of the IMPCHase active site of both avian and human ATIC (*1*).

MATERIALS AND METHODS

Materials. All reagents were obtained from Sigma-Aldrich, American Bioanalytical, VWR, or Fisher. FAICAR was prepared according to previously published procedures (*9*, *10*).

Construction of Site-Directed Mutants. All mutagenesis of human ATIC was performed using the QuikChange procedure (Stratagene, Inc.) using pETATIC-b (*8*) as the initial DNA template for all single mutants. Complementary primer sets (Table 1) were used to make the K66A, Y104A, Y104F, D125A, D125E, D125N, K137A, and K137R mutants. The double mutants Y104A/D125A and Y104F/D125A were constructed using the Y104A and Y104F primer sets and the D125A clone as the initial DNA template. The sequence of these mutant clones was verified by automated sequencing at the HHMI Biopolymer/W. M. Keck Foundation Biotechnology Resource Laboratory at Yale University.

Protein Expression and Purification. Both wild-type and mutant proteins were purified according to previously published procedures (*8*).

Identification of the Bound Purine in the Apo Avian ATIC Structure. Avian selenomethionine ATIC (provided by I. Wilson) was analyzed using HPLC to separate the bound nucleotide from the protein. ATIC along with XMP and GMP standards was separated on a Mono-Q anion exchange column (Amersham Biosciences, Inc.) using a linear gradient from 0 to 200 mM TEAB (pH 8.0). Mass spectrometry was then carried out on the unknown peak from the ATIC run using a Finnigan LCQ Deca instrument in the negative ion mode. Standards of XMP and GMP were also run as controls.

IMPCHase Activity Assay. Steady-state activity assays to determine the K_M and k_{cat} vales for each of the mutants were performed for a range of FAICAR concentrations. IMPCHase activity was followed by monitoring the formation of IMP at A_{248} on a Perkin-Elmer UV/Vis Lambda2 spectrophotometer with PECSS data acquisition software based on a previously reported method (*9*). All reaction mixtures were 500 μL in volume, and all reactions were performed in 100

Table 1: PCR Primers Used in Mutagenesis[a]

mutant	primers (5′ → 3′)
K66A	GAAATGTTGGGGGGACGTGTG**GCG**ACTTTGCATCCTGCAGTCCATG
	CATGGACTGCAGGATGCAAAGT**CGC**CACACGTCCCCCCAACATTTC
Y104A	GAGTTGTCGCCTGCAATCTC**GCG**CCCTTTGTAAAGACAGTGGC
	GCCACTGTCTTTACAAAGGG**CGC**GAGATTGCAGGCGACAACTC
Y104F	GAGTTGTCGCCTGCAATCTC**TTT**CCCTTTGTAAAGACAGTGGC
	GCCACTGTCTTTACAAAGGG**AAA**GAGATTGCAGGCGACAACTC
D125A	GCTGTGGAGCAAATT**GCG**ATTGGTGGAGTAACCTTAC
	GTAAGGTTACTCCACCAAT**CGC**AATTTGCTCCACAGC
D125E	GCTGTGGAGCAAATT**GAA**ATTGGTGGAGTAACCTTAC
	GTAAGGTTACTCCACCAAT**TTC**AATTTGCTCCACAGC
D125N	GCTGTGGAGCAAATT**GAT**ATTGGTGGAGTAACCTTAC
	GTAAGGTTACTCCACCAAT**ATC**AATTTGCTCCACAGC
K137A	CTGAGAGCTGCAGCC**GCA**AACCACGCTCGAGTG
	CACTCGAGCGTGGTT**TGC**GGCTGCAGCTCTCAG
K137R	CTTACTGAGAGCTGCAGCC**CGT**AACCACGCTCGAGTGACAG
	CTGTCACTCGAGCGTGGTT**ACG**GGCTGCAGCTCTCAGTAAG

[a] The mutations incorporated into the cDNA are bold and underlined.

mM Tris-HCl (pH 7.5) in a 1 cm path length quartz cuvette at room temperature (RT). Each assay was initiated with the addition of ATIC (final concentration of typically 10−700 nM) by rapid mixing of the cuvette. Stock protein concentrations were determined using Pierce Coomassie Plus protein assay reagent with bovine serum albumin as a standard. The data that were gathered were analyzed using the plotting and nonlinear regression curve-fitting program Kaleidagraph 3.5 (Synergy Software) by plotting FAICAR concentration versus velocity. The data were fit to the Michaelis−Menten equation to determine K_M and v_{max}. The values for k_{cat} were determined by dividing the value of v_{max} by the enzyme concentration used in the assay.

Solvent Isotope Effect on IMPCHase. A pH(D) range of 7.0−9.0 was used to compare the steady-state rate of wild-type ATIC with that of the Y104A mutant in H_2O and D_2O solutions. All reactions were assayed in 20 mM Tris-bis propane buffer made with double-distilled water or with 99% deuterium oxide. The pH was adjusted with concentrated HCl or NaOH. The pD was calculated by adding 0.4 to the reading from the pH meter to correct for the glass electrode solvent isotope artifact. The ionic strength at each pH(D) was kept constant at 100 mM using KCl. All assays were performed at RT under saturating concentrations of FAICAR. The differences in the steady-state rate in H_2O and D_2O over the entire pH(D) range were used to calculate the overall percent change in rate caused by the solvent isotope effect.

Enzyme Concentration Dependence Assays for K137A and K137R. Enzyme stock solutions ranging from 0.25 to 2 μM for the K137A and K137R mutants and ranging from 0.1 to 2.4 μM for wild-type ATIC were made to study the effect of enzyme concentration on the IMPCHase enzyme activity. The assays were performed as previously described (*8*) except the enzyme stocks were allowed to warm to RT for ~4 h, and assays were performed at RT.

Prediction of the Three-Dimensional Structure of FAICAR. FAICAR was drawn using the chemical structure program ChemDraw Standard, version 6 (Cambridge Software, Inc.), and then converted to a three-dimensional structure using Chem3D Professional, version 5.0 (Cambridge Software, Inc.). This three-dimensional structure was then energy minimized using their implementation of N. L. Allinger's MM2 force field (*11*, *12*).

Calculation of Partial Charges around Amide Nitrogens. Structures of FAICAR, acetamide, and acrylamide were drawn as described above using ChemDraw Standard. These were then used as inputs for AM1 molecular orbital calculations (*13*). Charges were calculated using the CM1 approach as described by Storer *et al*. (*14*). These calculations were carried out for us by W. Jorgensen (Department of Chemistry, Yale University).

RESULTS

There was some ambiguity with regard to the identity of the unknown ligand bound in the apo avian structure first published (*7*). The electron density narrowed the number of possible candidates to two molecules, XMP and GMP, but could not distinguish between them. HPLC analysis on avian ATIC revealed an unknown peak at 31.4 min, corresponding to the retention time of the XMP standard, while the GMP standard had a retention time of 19.7 min. To further verify that the bound nucleotide seen in the avian ATIC structure was indeed XMP, the unknown peak from HPLC was further studied using mass spectrometry. Both the XMP standard and unknown sample had molecular ion masses of 363.2 amu. From these two experiments and the fact that only GMP or XMP can be unambiguously modeled into the electron density of the unknown nucleotide in the apo avian structure, we believe the identity of the unknown nucleotide to be XMP.

Site-directed mutagenesis was carried out on the IMPCHase domain of human ATIC to determine the roles that residues Lys66, Tyr104, and Asp125 play in the IMPCHase reaction.[2] Mutants K66A, Y104A, Y104F, D125A, D125E, D125N, Y104A/D125A, and Y104F/D125A were constructed, and their effects on the steady-state kinetics were

[2] The experiments presented here were performed on human ATIC using the 1.75 Å avian crystal structure as a guide. The avian structure and human structure are structurally conserved, and possess an rmsd between their XMP-bound monomers of only 0.46 Å (*1*).

Table 2: Steady-State Results for ATIC Mutants[a]

	K_m (μM)	k_{cat} (s^{-1})	k_{cat}/K_m (M^{-1} s^{-1})
wt	0.9 ± 0.1	8.6 ± 0.2	1×10^7
K66A	115 ± 7	0.062 ± 0.001	5×10^2
Y104A	3.0 ± 0.3	0.136 ± 0.002	5×10^4
Y104F	3.6 ± 0.2	0.036 ± 0.001	1×10^4
D125A	9.1 ± 0.2	0.014 ± 0.001	2×10^3
D125E	5.2 ± 0.5	0.147 ± 0.001	3×10^4
D125N	2.7 ± 0.1	0.603 ± 0.004	2×10^5
K137A	31.0 ± 0.9	0.276 ± 0.003	9×10^3
K137R	2.7 ± 0.1	0.507 ± 0.004	2×10^5
Y104A/D125A	ND[b]	~0.001	–
Y104F/D125A	ND[b]	~0.0008	–

[a] The K_m, k_{cat}, and catalytic efficiency values for all site-directed mutants are summarized above. The errors were calculated from the errors from fitting the raw data to the Michaelis−Menten equation. The k_{cat} values for the double mutants were estimated by an IMPCHase activity assay using a saturating concentration of FAICAR. [b] Not determined.

determined. The results of these experiments are presented in Table 2 along with the values determined for wild-type ATIC.

Compared to wild-type ATIC, both of the Tyr104 mutants had very little effect on the K_M of FAICAR, suggesting that this residue plays only a minor role in substrate binding. The k_{cat} values for these mutants, however, suggest that this residue contributes significantly to catalysis. The Y104F mutant has a k_{cat} value that is 2 orders of magnitude lower than that of wild-type ATIC. Surprisingly, the Y104A mutant was more active than the Y104F mutant with a k_{cat} value that was only 1 order of magnitude lower than that of wild-type ATIC. This "rescue" by the Y104A mutant suggests that in the absence of the bulky phenol or phenyl group, water from bulk solvent can interact with FAICAR and participate in the reaction. To test this hypothesis, the solvent isotope effect on the IMPCHase steady-state rate was compared for wild-type ATIC and the Y104A mutant (Figure 3). The v_{max} rate for the IMPCHase assays carried out in D_2O for wild-type ATIC was reduced 27 ± 6% compared to the rate obtained in H_2O, while for Y104A, it was reduced 71 ± 1% compared to the rate obtained in H_2O. This difference indicates participation of solvent water in IMPCHase catalysis for the Y104A mutant and suggests that water can replace the function of the hydroxyl from Tyr104, although less efficiently.

The other residue in the proximity of FAICAR implicated in IMPCHase catalysis is Asp125. The D125A mutant had a K_m value that was 10 times greater than that of the wild type, suggesting that this residue contributes to substrate binding. Figure 2 supports this result, predicting that Asp125 interacts with the 2′- and 3′-hydroxyls on the ribose ring of FAICAR. There is also a reduction in the k_{cat} value of 2 orders of magnitude for the D125A mutant, suggesting that this side chain plays a significant catalytic role in the IMPCHase reaction. The D125E conservative mutant partially rescues the K_M and k_{cat} values. The K_M is not fully restored, presumably because of steric clashes with the ribose hydroxyl groups caused by the extra length and volume associated with the addition of a methylene group on the substituted side chain. The protein might itself adjust to accommodate the extra volume, or the conformation of FAICAR itself may be perturbed; in either case, the FAICAR may not bind in its optimum conformation or position. The

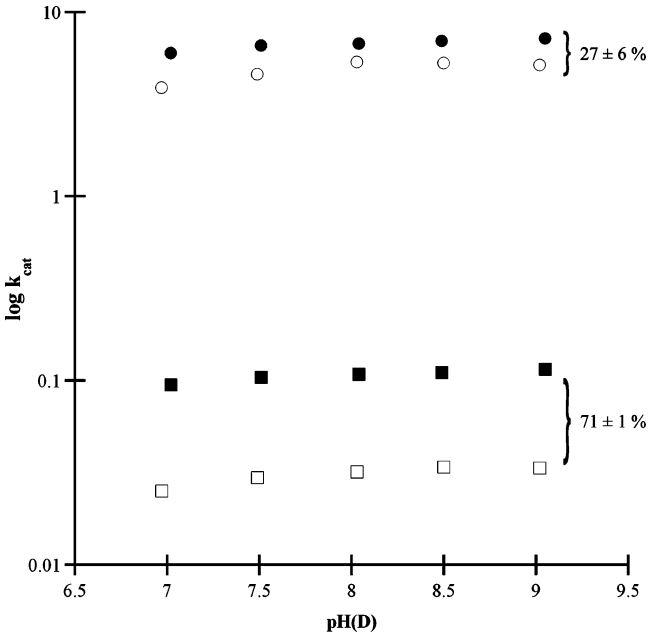

FIGURE 3: Solvent isotope effect on wild-type ATIC (● and ○) and Y104A (■ and □). The filled shapes represent data gathered in H_2O, and the empty shapes represent data gathered in D_2O.

nearly 60-fold decrease in the k_{cat} may also be explained by the same argument. If FAICAR is not in its optimal position for catalysis, the catalytic efficiency would be reduced. The D125N mutant almost fully restores the K_m value and also further rescues the k_{cat} value. Since the side chain of the D125N mutant can act only as a hydrogen bond donor or acceptor, this strongly suggests that Asp125 does not function as a general acid or base in the catalysis.

Interestingly, the Tyr104 and Asp125 mutants still possessed detectable IMPCHase activity. For this reason, double mutants Y104A/D125A and Y104F/D125A were constructed and assayed. The activities of both these double mutants were too low to determine K_m values, but the k_{cat} values were measurable (estimated to be 0.001 s^{-1} for the Y104A/D125A mutant and 0.0008 s^{-1} for the Y104F/D125A mutant). Since the uncatalyzed conversion of FAICAR to IMP cannot be detected in the reaction mixture in the absence of enzyme using the spectrophotometric assay, any absorbance change observed using this method results from the catalyzed reaction. The fact that even these double mutants still possess detectable IMPCHase activity clearly indicates that these residues alone are not sufficient to explain all of the catalytic effects of the IMPCHase site. The premise is that it is a combination of Tyr104 and Asp125 along with the numerous backbone interactions with FAICAR that are essential for efficient IMPCHase activity. A detailed structural look at these interactions is provided in Woland *et al.* (*1*).

The crystal structure of dimeric avian ATIC suggests that Lys137, from the opposite monomer chain, interacts with FAICAR through a water-mediated contact (*7*). It has been shown in our laboratory that although the dimeric form of ATIC is more active in catalyzing the IMPCHase reaction, the monomeric form also possesses IMPCHase activity (*8*). Therefore, this residue cannot be essential for catalysis of the IMPCHase reaction. The role of Lys137 was tested through mutagenesis and enzyme concentration dependence assays. The K137A mutant shows a large change in the K_m for FAICAR, with a value ~30-fold greater than that of the

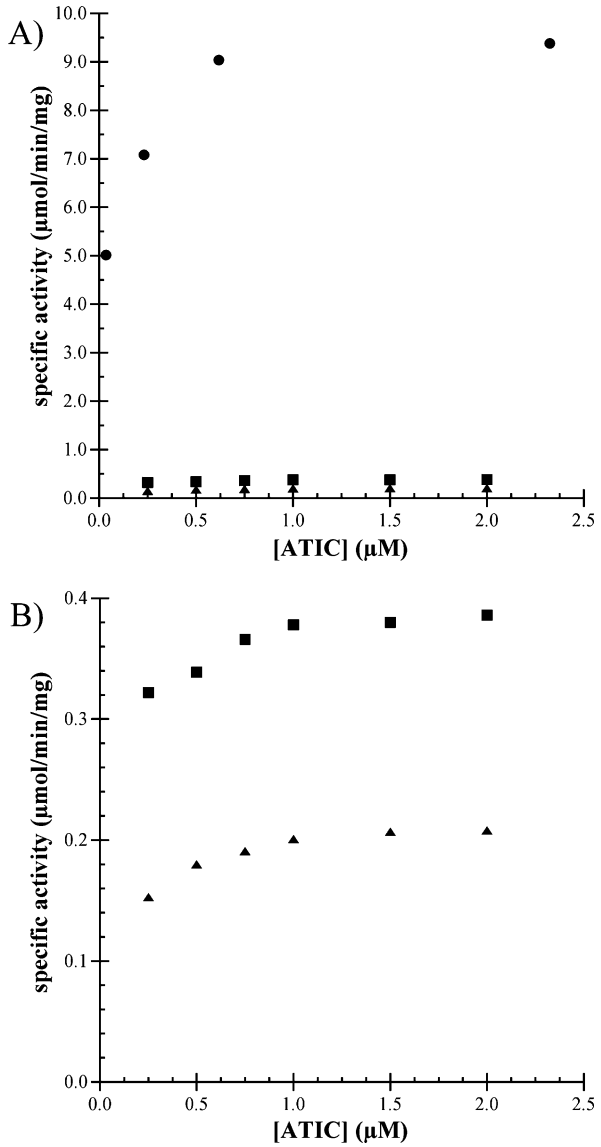

FIGURE 4: Enzyme concentration of wild-type ATIC (●), K137A (▲), and K137R (■) vs specific activity of the IMPCHase reaction shown at full scale (A) and at a decreased scale (B) to better show the K137A and K137R mutants.

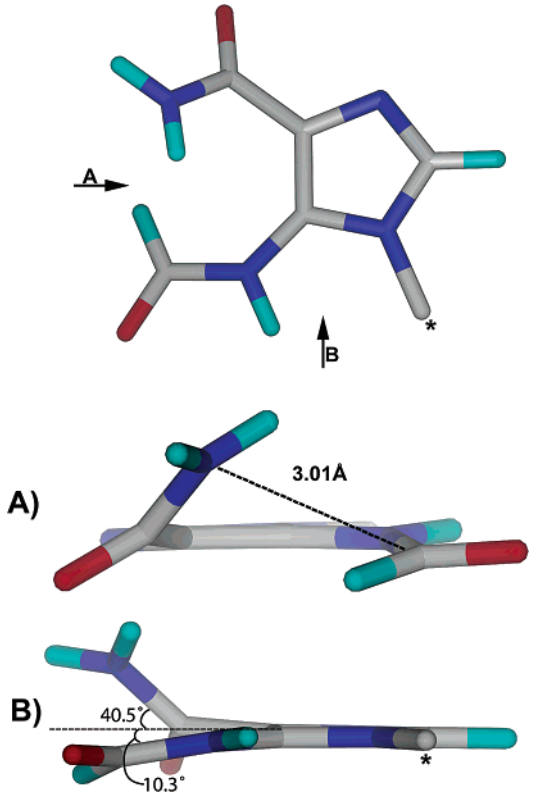

FIGURE 5: Energy-minimized structure of FAICAR predicted from MM2 force field calculations. Panels A and B represent views of the molecule along that direction. The asterisk represents the ribose phosphate that is not shown.

wild type. This suggests that Lys137 does, in fact, contribute to the binding of FAICAR. There is also a 30-fold decrease in the k_{cat} for the IMPCHase reaction, implying that this residue also may have a catalytic role when the protein is in its dimeric form. The conservative K137R mutation is able to rescue the K_m value but still displays a large decrease in the k_{cat} value. This mutation appears to be able to restore the proper binding of FAICAR but is not able to significantly contribute to catalysis of the IMPCHase reaction.

Concentration dependence assays of wild-type ATIC, K137A, and K137R were carried out to determine if these mutants still possess increased activity in the dimeric form of the enzyme. As Figure 4 shows, only wild-type ATIC shows a dramatic increase in specific activity with an increase in enzyme concentration. The two mutants displayed only a minimal concentration dependence. Unfortunately, the enzyme concentrations used for these concentration dependence experiments could not be correlated with the predicted fraction of ATIC dimer present since these data were gathered at RT and the monomer−dimer dissociation constant was obtained at 4 °C. Attempts to measure the dissociation constant were unsuccessful at 25 °C, because of the instability of ATIC at 25 °C in the analytical ultracentrifuge during the extended time required to complete the experiment. Also, attempts to gather accurate concentration-dependent kinetic data at 4 °C were unsuccessful due to the low activity of these mutants at this temperature. From these studies and the mutagenesis results, Lys137 is believed to be the origin of the increase in IMPCHase activity upon ATIC dimerization. Its effect on the overall efficiency of the reaction is marked.

The three-dimensional structure of FAICAR itself needs to be considered in postulating a mechanism for the IMPCHase activity. Using the Chem3D MM2 force field function, the structure of FAICAR was energy minimized using the "catalytically ready" form of FAICAR (i.e., with the carboxamide properly oriented for nucleophilic attack) as the initial input. Furthermore, this orientation of the carboxamide mimics how FAICAR is predicted to bind the IMPCHase active site based upon analysis of the active site in the XMP-bound ATIC structures (*1*). The energy-minimized structure from these calculations is shown in Figure 5. Despite the expectation that all atoms in the substituted imidazole moiety of FAICAR should be coplanar because of the sp^2 hybridization of the carbon and nitrogen orbitals, our calculations predict that the amide and formamide group of FAICAR will deviate from the plane of the imidazole ring of FAICAR by 40.5° and 10.3°, respectively. The results of molecular orbital and charge calculations are displayed in panels A and B of Figure 6. These calculations indicated that the partial charge around the 4-carboxamide

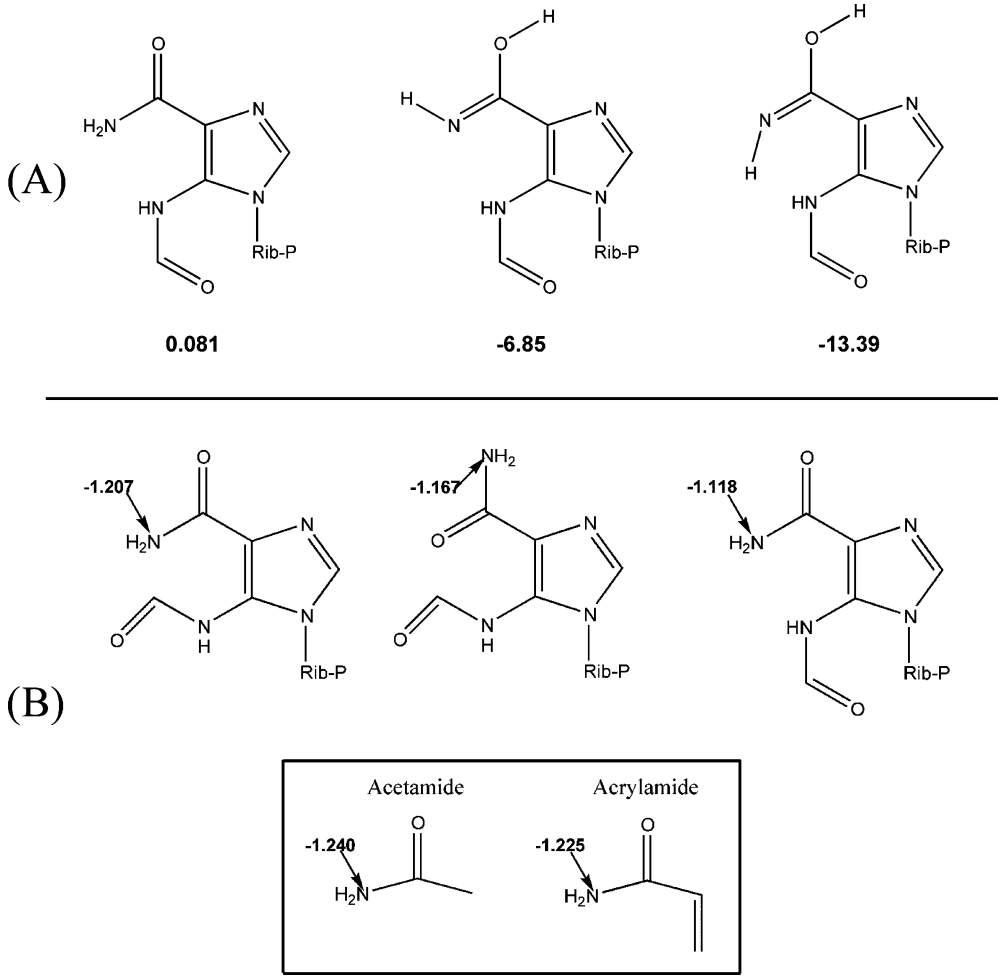

FIGURE 6: (A) Amide−imidol tautomerization of FAICAR. The calculated $\Delta H_{formation}$ (kilocalories per mole) values for each tautomer are shown. (B) Calculated partial charges around amide nitrogens. The model compounds are shown in the box.

nitrogen of FAICAR is likely to be somewhat smaller than the partial charges around the amide nitrogens of the model compounds, acetamide and acrylamide.

DISCUSSION

The availability of high-resolution structures of ATIC has suggested aspects of the IMPCHase catalytic mechanism of for study. Observations made from these structures point toward two amino acid residues, Tyr104 and Asp125, as likely candidates for participation in catalyzing the IMPCHase reaction since these residues are the only amino acids with the potential to act as catalytic residues which are in the proximity of the amide and formyl groups on FAICAR where the cyclization reaction occurs (Figure 2). Results from steady-state kinetic experiments on site-directed mutants of these two residues suggest that Tyr104 and Asp125 are important for the efficiency of the IMPCHase reaction but not absolutely required for catalysis. This is quite clearly demonstrated by the observation that double mutants of these residues still possess measurable IMPCHase activity. The importance of the hydroxyl group on the phenol ring of Tyr104 is demonstrated by the Y104F mutation which resulted in a 2 order of magnitude reduction in k_{cat} when compared to that of wild-type ATIC. Surprisingly, the Y104A mutant, in which the bulky phenolic ring is not present, demonstrates greater IMPCHase activity than the Y104F mutant. This aromatic ring is reported to bury FAICAR in the active site (*7*). When the aromatic ring is absent in the Y104A mutant, FAICAR becomes accessible to water from bulk solvent, which might replace the function of the hydroxyl normally present on Tyr104. The solvent isotope effect studies (Figure 3) support this hypothesis in that there is an only 27% reduction in the rate of wild-type ATIC between the IMPCHase reaction carried out in H_2O and D_2O, while there is a 71% rate reduction for the Y104A mutant.

Despite possessing a charged side chain, Asp125 does not appear to function in the IMPCHase reaction as a general acid and/or base. This is suggested by the observation that the D125N mutant displays an improved k_{cat} when compared to that of the D125A mutant. The side chain of asparagine is not ionized under physiologic conditions and can act only as a hydrogen bond donor and/or acceptor. This implies that Asp125 does not play a proton transfer role in the mechanism. A more likely possibility is that Asp125 is responsible for positioning FACIAR in the binding site. It is also possible that the negatively charged side chain could be responsible for stabilizing a partial positive charge generated in the transition state of the reaction. All of the other predicted protein−substrate interactions in the region of the ring closure reaction on FAICAR in the IMPCHase active site appear to be with the peptide backbone of ATIC, and are therefore cannot be tested by mutagenesis.

Located further away from the ring closure reaction, Lys66 was shown to be an important residue for both catalysis and

substrate binding. The 100-fold increase in K_M can easily be attributed to the loss of a positively charged side chain for binding the negatively charged phosphate of FAICAR. However, the 100-fold reduction in k_{cat} cannot be credited to the side chain of Lys66 participating directly in the ring closure reaction since this side chain is too far away to interact with amide or formyl groups on FAICAR. This effect can be attributed to improper positioning of FAICAR in the active site or to perturbation of the active site due to the loss of a positive charge. More likely, the reduction in k_{cat} is due to the loss of a basic side chain whose purpose is not only to bind FAICAR but also to interact and orient the hydroxyl group on Tyr104. As mentioned above, the side chain of Lys66 is within 3.5 Å of the hydroxyl group on Tyr104, whose hydroxyl was shown to be important for catalysis. Proper orientation of the hydroxyl group for proton abstraction during catalysis would be necessary for efficiency. Furthermore, the proximity of a highly basic, positively charged side chain to the hydroxyl of tyrosine would favor proton abstraction for generation and stabilization of a negatively charged oxyanion on Tyr104. Since an increasing pH would make the proton on the Tyr104 hydroxyl more labile, it is expected that activity would also increase as a function of pH. This trend was shown to be true in wild-type ATIC (*5*). In addition, unpublished preliminary data from our laboratory on the effect of pH on the activity of the K66A mutant support this in that as the pH is increased, the activity of this mutant increases exponentially.

Likely IMPCHase mechanisms involve a nucleophilic attack of the amide nitrogen on the formyl carbon of FAICAR. However, amide nitrogens are normally relatively poor nucleophiles due to resonance delocalization of electrons. This resonance stabilization of amides causes the lone pair of electrons on the nitrogen to be shared with the adjacent carbonyl group, thus sequestering them from participating in a nucleophilic attack. One means by which the nucleophilicity of the amide nitrogen might be enhanced is through amide−imidol tautomerization (Figure 6A). Ordinarily, the amide forms of such tautomers are strongly favored; however, the imidol form may be favored through formation of a conjugated system and/or intramolecular hydrogen bonding, each of which is possible in the case of FAICAR. It is also possible that interactions with the enzyme catalytic site might further stabilize the imidol tautomer of FAICAR. Nevertheless, energy calculations on these two tautomers predict that the imidol form of FAICAR would be much less stable than the amide form.

FAICAR possesses a conjugated electronic arrangement which might free the lone pair of electrons of the amide nitrogen and thus enhance its nucleophilicity. The extent to which canonical resonance forms of FAICAR contribute to its overall electronic structure would be an important determinant of the nucleophilicity of the amide nitrogen of FAICAR. To explore this possibility, we carried out molecular orbital calculations to estimate the partial charge around this amide nitrogen. The results of these calculations, depicted in Figure 6B, strongly suggest that enhanced partial charge around the FAICAR amide nitrogen is unlikely, as the calculated values are actually less than those calculated for the model compounds, acetamide and acrylamide. These results are consistent with the usual view of the imidazole ring system as electron-withdrawing.

Perhaps the simplest way in which the amide nitrogen of FAICAR might become more nucleophilic is through deprotonation. The pK_a values of model compounds acetamide and benzamide are 15.1 and 13, respectively (*15*). These values might suggest that deprotonation of the FAICAR amide nitrogen would only occur in the presence of a strong base. No such base is apparent in the IMPCHase active site of ATIC. However, the pK_a values of FAICAR have previously been reported (pK_{a2} = 5.81 ± 0.03 and pK_{a3} = 9.41 ± 0.04). The value of pK_{a2} was assigned to the second ionization state of the 5′-phosphate group, and pK_{a3} was assigned to the dissociation of the proton at C-2 on the imidazole ring of FAICAR (*5*). ^{1}H NMR spectra of AICAR and IMP determined in water at pH 7 and 12 using a water suppression scheme showed clearly that neither the C-2 proton of AICAR nor the analogous C-8 proton of IMP dissociates in these related molecules (data not shown). It is therefore more plausible that pK_{a3} should be assigned to dissociation of the proton of the amide nitrogen of FAICAR. As mentioned above, the electron withdrawing properties of the imidazole ring system would favor deprotonation of the amide nitrogen and result in a lower than expected pK_a value. This pK_a value is more permissive for deprotonation of the amide nitrogen at physiological pH, thus allowing for nucleophilic attack on the formyl carbon. In addition, the observation that FAICAR is converted spontaneously to IMP at high pH provides further evidence to support amide deprotonation as an element of the cyclization reaction and is consistent with previously reported results (*9*).

It is plausible that a major role of the IMPCHase active site is primarily to orient the substrate in the binding pocket in a configuration which favors the intramolecular ring closure reaction. Consistent with this notion is the observation that all of the predicted interactions of FAICAR and the IMPCHase active site shown in Figure 2 involve amino acid residues which have been conserved throughout evolution, except for two semiconserved interactions with the ribose hydroxyls as determined from the sequence alignments of various eukaryotic and prokaryotic ATICs (data not shown). Positioning of the substrate by the enzyme may be an example of an orbital steering mechanism. Koshland (*16*) proposed this type of mechanism in which he postulated that the precise angular arrangement of reactants and the "steering" of the reactants during the reaction are important for the catalytic power of enzymes. On the basis of the idea that an attacking nucleophile must approach from above or below the plane of a carbonyl at an angle of approximately 109° (*17*, *18*) and that the electrons from the nucleophile must be added to the empty π^* orbital (*17*, *19*), successful attack requires that FAICAR not be planar as the ring closure reaction occurs. Energy minimization calculations on FAICAR predict this to be the case (Figure 5) in that the imidazole ring of FAICAR is planar but both the amide and formyl portions of FAICAR lie outside the imidazole plane. Thus, even prior to binding to the enzyme IMPCHase site, FAICAR may be partially oriented to favor intramolecular cyclization. The angle between the amide nitrogen and carbonyl carbon is not at the predicted optimum angle for nucleophilic attack. Further orientation by the IMPCHase active site might be required to achieve the proper angle. The positioning of the reacting groups of FAICAR in the

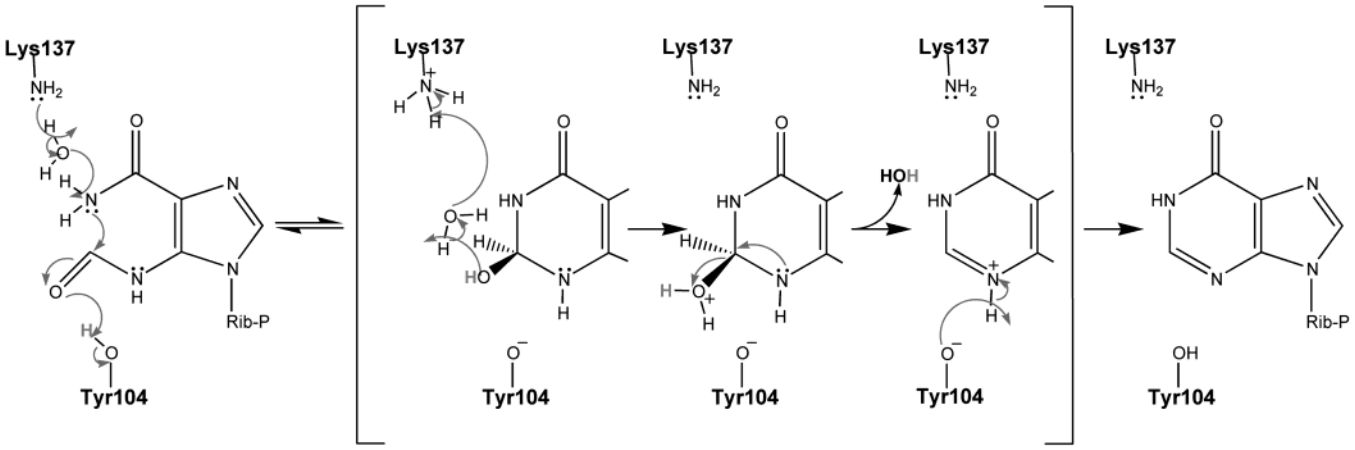

FIGURE 7: Proposed mechanism for the IMP cyclohydrolase reaction of ATIC. Lys137 is located on the other monomer of the protein and thus only present in the dimeric form of the enzyme.

proper orientation for nucleophilic attack would then be expected to enhance the reaction rate.

The mutagenesis and kinetic studies on Lys137 suggest that this residue is responsible for the increase in enzymatic activity seen in the dimeric form of the protein observed in previous studies (*8*). The side chain of Lys137 is too far away to directly interact with FAICAR, but it could exert its influence through bridging water molecules, which were resolved in the crystal structure (*7*). Lys137 is important for optimal binding of FAICAR as seen by the change in the K_M for the K137A mutant. Surprisingly, the conservative K137R mutant was not able to restore the enzyme concentration dependence seen in the IMPCHase activity and was only able to restore the K_M for FAICAR. This suggests that the K137R mutant was able to restore the binding affinity for FAICAR but is unable to keep the IMPCHase domain in its more active conformation. This is probably a result of the water interactions between this side chain and FAICAR being disrupted or coordinated differently in this mutant and the wild-type lysine. Without the catalytic water molecule(s) properly coordinated to a residue that can act as a general acid and base, the reaction rate would be slowed compared to the wild-type rate. The importance of Lys137 in enhancing the IMPCHase reaction in the dimeric form is seen in the 4 order of magnitude decrease in catalytic efficiency in the K137A mutant.

From the results and observations presented in this paper, a mechanism for the IMPCHase reaction is postulated in Figure 7. Initially, a proton is abstracted from the 4-carboxamide of FAICAR. In the dimeric form of ATIC, this would be accomplished by Lys137 on the other monomer via a water conduit. The coordination of Lys137 from the other monomer with water allows the greater catalytic efficiency observed in the dimeric form of the protein (*8*) to be explained since this residue would be able to more efficiently abstract the amide proton from FAICAR. In the monomeric form, this initial proton abstraction would have to be performed by bulk solvent and would occur much less efficiently and thus at a slower rate. The electron withdrawing properties of the imidazole ring are predicted to make the loss of the amide protein more favorable for both the monomeric and dimeric form of ATIC. The IMPCHase reaction then almost certainly proceeds through the tetrahedral aminol intermediate formed by nucleophilic attack by the FAICAR 4-carboxamide nitrogen on the carbonyl carbon of the adjacent 5-formamido group to close the purine ring. This reaction has a number of factors which tend to favor it kinetically. It is an intramolecular process, thus favored entropically (*20*); it forms a relatively strain-free six-membered ring; and this ring can readily aromatize. After the initial proton abstraction, the rest of the mechanism involves mostly proton transfers. The proton transfer steps in this mechanism should not be treated as a detailed path from substrate to product since there are many ways proton shuffling can occur to form IMP from FAICAR. During the course of this chemical reaction, one proton from Tyr104 and another from bulk solvent are donated to FAICAR, forming a leaving group of water on the formyl carbon. The Tyr104 hydroxyl is regenerated by the removal of the amine proton from the IMP intermediate. No matter what the specific path(s) of the reaction, the data presented here and in Woland *et al*. (*1*) strongly suggest that it is the orientation and binding of FAICAR in the IMPCHase active site, not the catalytic potential of the side chains, that are most important for the efficient conversion of FAICAR to IMP.

ACKNOWLEDGMENT

We thank Karen Anderson, Karen Bulock, Don Engelman, Dieter Söll, and Scott Strobel of Yale University; Samantha Greasley, Ian Wilson, and Dennis Wolan of the Scripps Research Institute (La Jolla, CA); and Jay Davies of Agouron Pharmaceuticals for helpful discussions throughout the duration of this project. Furthermore, we particularly thank William Jorgensen of Yale University for performing the molecular orbital calculations and Tomek Cierpicki and John Bushweller of the University of Virginia (Charlottesville, VA) for their assistance with the NMR experiments.

REFERENCES

1. Wolan, D. W., Cheong, C., Greasley, S. E., and Wilson, I. A. (2004) *Biochemistry 43*, 1171−1183.
2. Smith, J. L. (1995) *Curr. Opin. Struct. Biol. 5*, 752−757.
3. Kondo, M., Yamaoka, T., Honda, S., Miwa, Y., Katashima, R., Moritani, M., Yoshimoto, K., Hayashi, Y., and Itakura, M. (2000) *J. Biochem. 128*, 57−64.
4. Graupner, M., Xu, H., and White, R. H. (2002) *J. Bacteriol. 184*, 1471−1473.
5. Szabados, E., Hindmarsh, E. J., Phillips, L., Duggleby, R. G., and Christopherson, R. I. (1994) *Biochemistry 33*, 14237−14245.

6. Wolan, D. W., Greasley, S. E., Beardsley, G. P., and Wilson, I. A. (2002) *Biochemistry 41*, 15505−15513.
7. Greasley, S. E., Horton, P., Ramcharan, J., Beardsley, G. P., Benkovic, S. J., and Wilson, I. A. (2001) *Nat. Struct. Biol. 8*, 402−406.
8. Vergis, J. M., Bulock, K. G., Fleming, K. G., and Beardsley, G. P. (2001) *J. Biol. Chem. 276*, 7727−7733.
9. Mueller, W. T., and Benkovic, S. J. (1981) *Biochemistry 20*, 337−344.
10. Shaw, G., and Wilson, D. V. (1962) *J. Am. Chem. Soc. 84*, 2937−2940.
11. Allinger, N. L. (1977) *J. Am. Chem. Soc. 99*, 8127−8134.
12. Allinger, N. L., Yuh, Y. H., and Lii, J. H. (1989) *J. Am. Chem. Soc. 111*, 8551−8566.
13. Dewar, M., Zoebisch, E., Healy, E., and Stewart, J. (1985) *J. Am. Chem. Soc. 107*, 3902−3909.
14. Storer, J. W., Giesen, D. J., Cramer, C. J., and Truhlar, D. G. (1995) *J. Comput.-Aided Mol. Des. 9*, 87−110.
15. Lide, D. R. (2001) in *CRC Handbook of Chemistry and Physics*, CRC Press, Cleveland.
16. Storm, D. R., and Koshland, D. E. (1970) *Proc. Natl. Acad. Sci. U.S.A. 66*, 445−452.
17. Dunitz, J. D. (1995) *X-ray Analysis and the Structure of Organic Molecules*, Verlag Helvetica Chimica Acta, Basel, Switzerland.
18. Burgi, H. B., Dunitz, J. D., and Shefter, E. (1973) *J. Am. Chem. Soc. 95*, 5065−5067.
19. Kirby, A. J. (1996) *Stereoelectronic Effects*, Vol. 36, Oxford University Press, Oxford, U.K.
20. Bruice, T. C., and Lightstone, F. C. (1999) *Acc. Chem. Res. 32*, 127−136.

BI035139B